Self-Assembly and Reconfigurability of Shape-Shifting Particles

Trung Dac Nguyen,[†] Eric Jankowski,[†] and Sharon C. Glotzer[†,‡,*]

[†]Department of Chemical Engineering and [‡]Department of Materials Science and Engineering, University of Michigan, Ann Arbor, Michigan 48109, United States

ABSTRACT Reconfigurability of two-dimensional colloidal crystal structures assembled by anisometric particles capable of changing their shape were studied by molecular dynamics computer simulation. We show that when particles change shape on cue, the assembled structures reconfigure into different ordered structures, structures with improved order, or more densely packed disordered structures, on faster time scales than can be achieved *via* self-assembly from an initially disordered arrangement. These results suggest that reconfigurable building blocks can be used to assemble reconfigurable materials, as well as to assemble structures not possible otherwise, and that shape shifting could be a promising mechanism to engineer assembly pathways to ordered and disordered structures.

KEYWORDS: reconfigurable materials · self-assembly · shape-shifting particles · computer simulation

Next generation materials will be distinguished by their ability to adapt in novel ways both on demand and to environmental cues to perform important functions. The ability of materials to carry out molecular recognition, autonomous sensing and reporting, and to change properties when needed, all require that intrinsic building blocks be able to reconfigure from one structure to another. While adaptability is ubiquitous in biological systems, few if any examples of this ability can be found in traditional synthetic materials. For instance, it is well-known that proteins, the basic building blocks of biology, are the canonical switchable particle with a configuration that is entirely dependent upon solvent pH, the presence of ligands, and the presence of other proteins. Numerous studies have recently been conducted in attempts to mimic such protein-like switchability in nano- and microscale systems with implications to adaptive, functional materials. An interesting model of switchable self-assembling objects was developed recently by Bishop *et al.*[1] They studied the formation of hexamers of triangular robotic pucks, which are able to move on an air hockey table and detach from/attach to other pucks. Klavins *et al.* utilized this model to demonstrate how switchable components can be used to direct the assembly of a target structure.[2]

Today's materials are primarily static: once formed they retain the same structure throughout their lifetime, aside from aging, fatigue, corrosion and other deleterious effects. Shape memory alloys remember their original shape and after deformation can return to it through rearrangement of the constituent atoms *via* heating. Only recently have techniques become available to consider the synthesis and fabrication of dynamically switchable nanoparticle-based materials, that is, materials whose structure can dynamically reconfigure between two or more states through controlled changes of the nanoparticle itself. Materials self-assembled from shape-changing building blocks could be among the first experimentally realized materials in this class. For example, experiments have shown that colloidal gold nanorods can be shortened or shifted to other shapes such as spheres, bent, twisted, or ϕ-shaped by using laser pulses with different wavelengths and widths.[3−5] As the colloidal particles change shape from rodlike to spherical, their packing pattern transforms from nematic to triangular lattices accordingly.[3−5] The transformations, however, were irreversible. Kim *et al*. reported thermally responsive capsule structures with 25 nm diameter pores on the shell formed by hierarchical self-assembly of double tethered rod amphiphiles. Upon heating or cooling, the hydrophilic oligo-(ethylene oxide) coils at one end of the rods shrink or expand, respectively, resulting in a reversible closed/open gating motion of the nanopores.[6] They also demonstrated a reversible transformation between two-dimensional sheets and tubular structures assembled by laterally grafted rod amphiphiles upon heating *via* a similar mechanism.[7] Alternatively, polypeptide-based block copolymers can also be used as stimuli responsive building blocks due to the ability of the polypeptide segments to

* Address correspondence to sglotzer@umich.edu.

Received for review August 10, 2011 and accepted September 27, 2011.

Published online September 27, 2011
10.1021/nn203067y

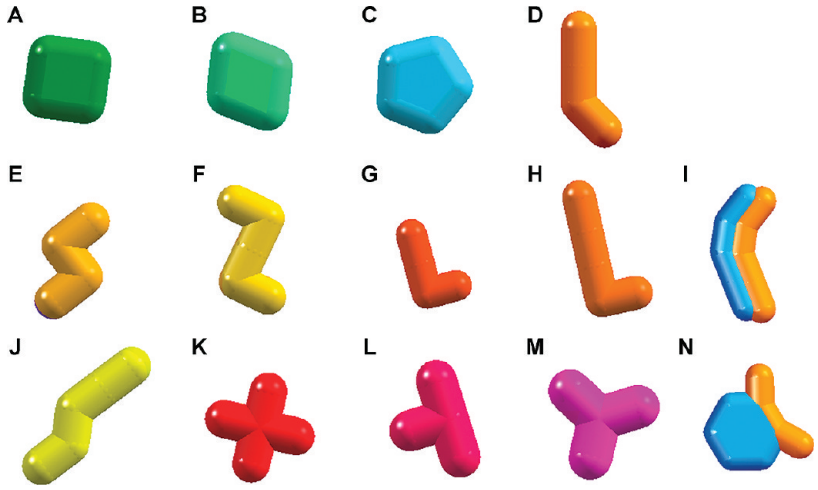

Figure 1. Model target shapes for shape-shifting from spheres (or equivalently, circles in 2-D simulations) and from rods. Convex shapes: (A) square; (B) rhombus; and (C) pentagon. Nonconvex shapes: (D) hockey stick H4; (E) zigzag Z4; (F) zigzag Z5; (G) L-shaped L4; (H) L-shaped L5; (I) bow-shaped B5, (J) sheared zigzag SZ5; (K) cross-shaped C5; (L) T-shaped T4; (M) Y-shaped particles Y4; and (N) "bull-head" B8. Shapes I and N are inspired by recent experimental studies on morphing PLGA-based biphasic rods.[12] The trailing number indicates the number of constituent, overlapping spheres (N_B) used to model each particle. Particles are drawn smooth.

adapt various conformations.[8−10] Gebhardt *et al*. demonstrated that the polypeptide rod segment in the poly(butadiene)-poly(L-lysine) block copolymers undergoes an α-helix−coil transition in response to a change in pH and temperature.[10] Yoo *et al*. synthesized polymeric particles that are able to switch shape in response to changes in temperature, pH, and chemical additives.[11] Recent experiments demonstrate that biphasic rods based on poly-(lactic-*co*-glycolic acid) (PLGA) are able to morph into various shapes, for example, bows, lemons, and "bull heads", upon heating one of the polymeric compartments above its glass transition temperature.[12] Given the variety of diverse nano- and colloidal particle shapes now available,[13] fabricating particles from materials that allow a reversible shape change upon application of an external stimulus, such as a laser pulse, could enable the assembly of a vast number of reconfigurable materials. For example, polymeric nanorods comprising an anisotropically cross-linked gel could be made to swell or contract lengthwise. Other more complex geometry changes may also be envisioned.[14,15]

Although the morphology of assembled structures strongly depends upon the comprising building block shape,[16−20] little is known regarding the response of those structures as the building blocks change shape. Batista *et al*. studied the crystalline packing of deformable spherical colloids.[21] The model spherical particle can continuously change shape into prolate or oblate ellipsoids, allowing for higher packing fractions than hard spheres in a fixed volume. Furthermore, the system was shown to undergo a second transition to an orientationally ordered crystal upon shape shifting. Recently, Zhang and co-workers demonstrated that a simple cubic lattice of palladium nanocubes coated by dodecanethiol ligands in toluene, a poor solvent for the ligands, transforms into a rhombohedral lattice upon solvent evaporation. Shifting of the nanoparticle shape from cuboid to ellipsoid was attributed to the swelling ligands as the solvent concentration decreased during evaporation.[22] In a previous study, we showed that when rod segments of oligomer-tethered nanorods are abruptly shortened or lengthened, the assembled structure reconfigures between a rectangular grid and bilayer sheets.[23] We also found that the reversible transformation between these two structures completes substantially faster than self-assembly due to their common substructure, that is, the bilayer ribbons.[23] These seminal results clearly suggest the potential power of shape-changing building blocks for reconfigurable materials.

Here we seek to develop an intuitive framework for investigating assemblies of nano- and microbuilding blocks whose shape can be dynamically shifted using external stimuli. Using a phenomenological model of attractive rigid particles that can transform on cue into predefined shapes (Figure 1) during a Brownian dynamics simulation, we study a set of switching scenarios to elucidate the relationship between shape-shifting building blocks, assembly of target structures, and structural reconfigurability among target structures. For illustrative purposes, we restrict our studies here to assemblies of particles in two dimensions; our simulation framework can be easily extended to 3-D systems, as illustrated in our previous study.[23] The particles are initialized in preassembled, two-dimensional ordered structures (Figure 2), and then uniformly transformed into different shapes. We demonstrate that by changing the building block shape (1) free-energy minimizing structures can be assembled more

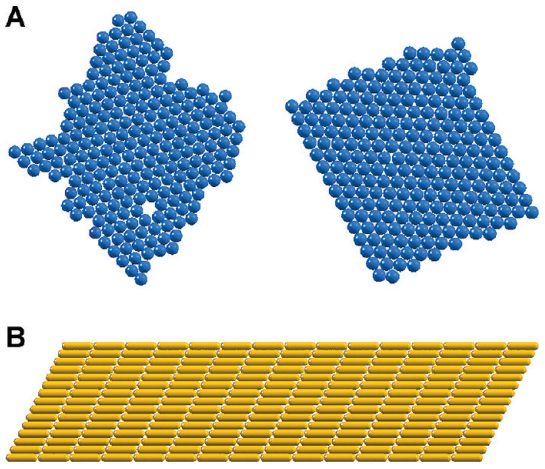

Figure 2. Preordered structures: (A) spheres preordered in triangular lattices obtained from self-assembly (left) and from artificially initializing (right). (B) rods preordered in a smectic-like structure. Rods are drawn as smooth for visual clarity.

efficiently and with fewer defects than self-assembly from disordered states; (2) unexpected ordered structures can emerge; and (3) ordered assemblies can be reconfigured. These results serve to inspire novel approaches to the fabrication of adaptive nanomaterials as well as to engineering assembly pathways to structures that are inaccessible *via* traditional assembly methods. Because the specific shapes we consider can be fabricated today, and in some cases (described herein) shape changing is already possible, the results presented here are achievable now and should serve to motivate experiments on these novel systems.

RESULTS AND DISCUSSION

The initial ordered configurations are prepared by performing thermodynamic self-assembly simulations of spheres or rods either from disordered initial states or from preordered initial states (see Methods). For the systems prepared from disordered states, the largest ordered aggregates are extracted and subsequently put into a larger simulation box where shape transformation of the particles is triggered. Our results indicate that in many cases the shape shifting not only enhances the formation of ordered structures from the target shape particles over their self-assembly from disordered states, but also allows for the reconfiguration between these ordered structures and their initial structures. This enables one to design multiple-step assembly of desired ordered structures, which are unattainable from conventional assembly methods. Here we define reconfigured structures as those resulting from shifting the particle shape, and self-assembled structures as those formed from isotropic states by particles in the target shape.

Efficient Assembly. Table 1 shows that when spheres and rods preassembled in ordered structures are shifted into other shapes, the target particles form

TABLE 1. Resulting Structures from Shifting Spheres and Rods

	target shape		
initial shape (initial ordered structure)	convex	rodlike	branched
spheres (triangular lattice)	ordered	disordered	ordered*
rods (smectic structure)	ordered	ordered	ordered*

* Except T-shaped particles.

ordered structures in most cases. For target shapes that are convex (*e.g.*, squares, rhombuses, and pentagons), or rodlike (*e.g.*, zigzags Z5 and hockey sticks H4), or symmetric and branched (*e.g.*, Y-shaped and cross-shaped particles), the preordered structures reconfigure to ordered structures that are predictable for particles of that shape (Figure 3). In contrast, when these particles self-assemble from initially disordered, low density states, many are prone to falling into kinetic traps, resulting in a small correlation length of the ordered domains. To avoid such kinetic traps, the system should be slowly cooled and/or compressed as in experiments and conventional self-assembly simulations, and even then kinetic traps may be unavoidable, especially for those particles with steric anisotropy. Meanwhile, the rearrangement of particles from preordered configurations as they transform to target shapes allows for the formation of ordered domains with correlation lengths comparable to that of the initial configurations.

For example, when spheres in a triangular lattice morph into squares, their hexagonally packed nearest neighbors help maintain the close-packing of the lattice while the square shape guides the packing into a rectangular lattice (Figure 3A). Similarly, the rhombuses transformed from either spheres or rods form the same crystalline structure (Figure 3B), as do pentagons (Figure 3C). Likewise, when cross-shaped particles are either grown from spheres or transformed from rods, they easily interleave with their neighbors (Figure 3D). The local ordering of the reconfigured structures for these target shapes is identical regardless of the initial particles and configurations. T-shaped particles, however, are an exception due to their asymmetry. It should be noted that in certain cases the packing pattern of reconfigured structures is largely driven by the "bumpiness" of our model particles (see the Methods section), for example, for squares (Figure 3A) and rhombus particles (Figure 3B). For other cases, the "bumpy" particles are able to pack into similar patterns to those predicted for smooth hard particles (Figure 3C–F). Interestingly, the pentagons (Figure 3C) exhibit a similar crystalline ordering observed in hard pentagon systems.[24]

Rodlike particles such as hockey sticks, zigzags, and L-shaped particles rarely assemble into long-range ordered structures from initially disordered states

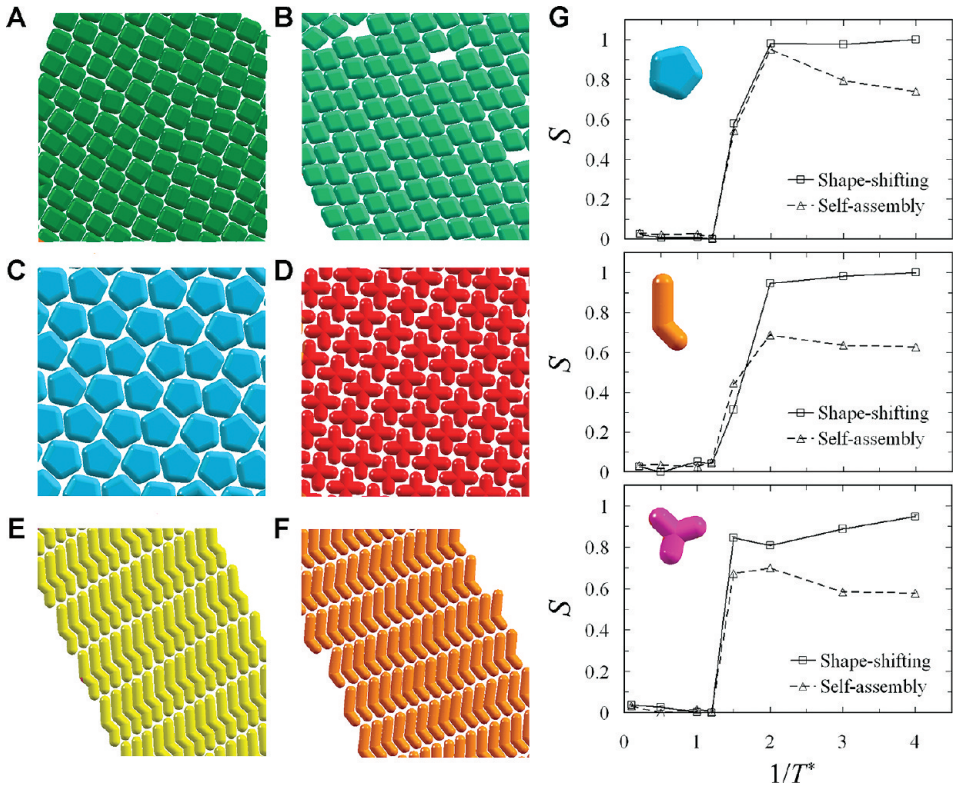

Figure 3. Ordered structures by shifting particle shape from (A) sphere to square; (B) rod to rhombus; (C) sphere to pentagon; (D) sphere to cross; (E) rod to sheared zigzag SZ5 and (F) rod to hockey H4. Snapshots are taken from systems of $N_P = 225$ particles. (G) Comparison between reconfigured and self-assembled structures using shape-matching order parameters at different inverse temperatures for three different target particle shapes. Particles aggregate when $1/T^* > 1.2$. The self-assembled structures are obtained from a fast quench from disordered states. The error bars, which are smaller than the symbols, are standard deviations from the mean value measured from 20 independent samples. Particles are drawn as smooth for visual clarity.

because of their steric anisotropy. For these rodlike particles to reach their thermodynamically stable state, they typically need to be driven by an external field, or gradually annealed with a significant amount of time to relax into ordered structures, and even then kinetic traps may be unavoidable in practice. However, when these anisotropic particles are transformed from preordered rods, which are geometrically similar and easy to order *via* self-assembly, the ordered structures we desire from self-assembly emerge spontaneously. For example, when hockey sticks H4 and sheared zigzags SZ5 result from "bending" preordered rods, the presence of initial smectic layers guides the particles to nest with their adjacent neighbors in the same layer, leading to polar smectic structures (Figure 3D and 3E). As a result, crystalline structures can emerge without any change in thermodynamic parameters like pressure or temperature.

We employ the general shape-matching algorithm developed by Keys *et al.*[25] to compare the resulted structures from shape transformation/reconfiguration and those from self-assembly with corresponding target shapes (see the Methods section). Figure 3G shows the order parameter of pentagons, hockey sticks, and Y-shaped particles, representative of convex, rodlike, and nonconvex shapes, as functions of inverse temperature, or equivalently, the attraction strength between the particles. We found that for nonconvex target shapes (including rodlike shapes) the transition into ordered structures was much sharper as they underwent shape transformation than it was for self-assembly. At higher temperatures, the difference between reconfigured and self-assembled structures is insignificant because the systems are all in isotropic states. At low temperatures, self-assembled structures from Y-shaped particles, hockey sticks ($1/T^* > 1.2$) and pentagons ($1/T^* > 2.0$ or $T^* < 0.5$) suffer from kinetic traps, and hence have more defects than the counterpart structures generated from shape-shifting. From Figure 3G, we identify a critical temperature, $1/T^* = 1.2$ for nonconvex shapes and $1/T^* = 2.0$ for convex shapes, in our model system, below which the shape-shifting induced reconfiguration is advantageous over self-assembly from disordered states with longer-range ordering and shorter relaxation times.

When rodlike particles such as hockey sticks, zigzags, and L-shaped particles are grown from spheres, the resulting structures do not exhibit smectic-like ordering as they did when transformed from rods (Figure 4). This is because the directionality inherent

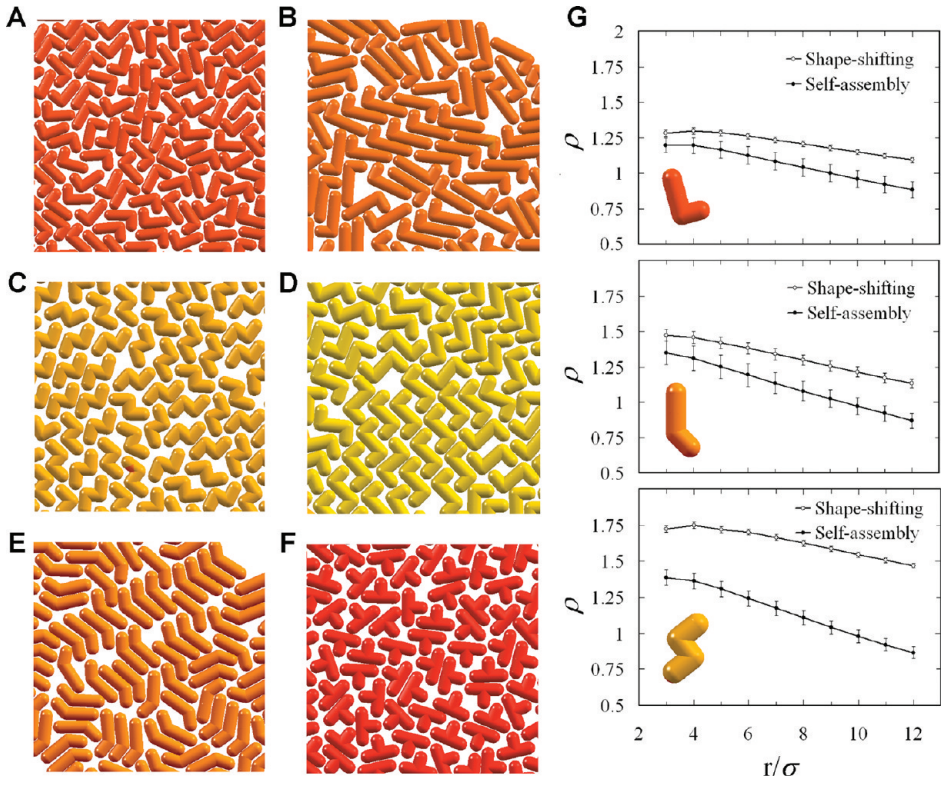

Figure 4. Disordered structures obtained from transforming spheres into (A) L-shaped L4; (B) L-shaped L5; (C) zigzags Z4; (D) zigzags Z5; (E) hockey sticks H4; and (F) T-shaped particles. Particles are drawn as smooth for visual clarity. Snapshots are taken from systems of $N_P = 225$ particles. (G) Comparison between reconfigured and self-assembled structures in terms of the average local number density ($\rho = N/F$, where N is the number of beads and $F = 4\pi r^2$ is the circular area surrounding any given particle within a distance r, averaged over the whole sample). Particles aggregate for $1/T^* > 1.2$. The self-assembled structures are obtained from an instantaneous quench from disordered states. The error bars are standard deviations from the mean value measured from 20 samples.

to the triangular lattice of spheres does not favor the smectic ordering present in rod layers. Here, the only visual difference between reconfigured and self-assembled structures is the local packing density of particles. For some representative nonconvex shapes (Figure 4A–F), the local density of reconfigured structures is remarkably higher than that in self-assembled structures at $T^* = 0.2$, again due to the initial close-packed configuration (Figure 4G). These results suggest that for nonconvex shapes, particularly those with highly anisotropic geometry, choosing a good candidate for the initial shape and preordered configuration, for example, with favorable directionality, is crucial to stabilizing final ordered structures.

Inspired by recent experiments in which submicrometer-sized biphasic rods of poly-(lactic-*co*-glycolic acid) (PLGA) can be bent into bows or morphed into "bull-head" shapes as the temperature is raised above the glass transition of one of the two polymeric components,[12] we perform simulations to predict the behavior of different rod assemblies under such shape transformations. From the experimental data,[12] it is reasonable to assume that the attractions between the compartments from different rods (yellow–yellow, blue–blue, and blue–yellow) are equally strong. When the bow-shaped particles self-assemble, the resulting structure is disordered (Figure 5A) and trapped in a kinetically arrested state. Meanwhile, a smectic structure preassembled by rods reconfigures into another smectic structure when the rods bend on cue into bows (Figure 5B). In this case, the reconfigured structure is more preferred than the self-assembled counterpart both energetically and entropically at the same temperature ($T^* = 0.2$).

Likewise, when the rods are transformed to "bull-head" shapes, the reconfigured structure is more ordered than its self-assembled counterpart at the same temperature (Figure 5C,D). The ordered structures cannot be attained *via* our self-assembly simulations even with a slow cooling schedule due to the highly concave geometry of the particles, which causes extreme steric traps. This example, again, illustrates how shape shifting allows for more efficient assembly than the traditional self-assembly procedure.

Pathways to Unexpected Ordered Structures. Although ordered crystals of convex shape particles can be achieved *via* self-assembly, those of nonconvex particles are more challenging because of steric restrictions, or are prone to kinetic traps and prohibited by many competing local energy minima. We have previously

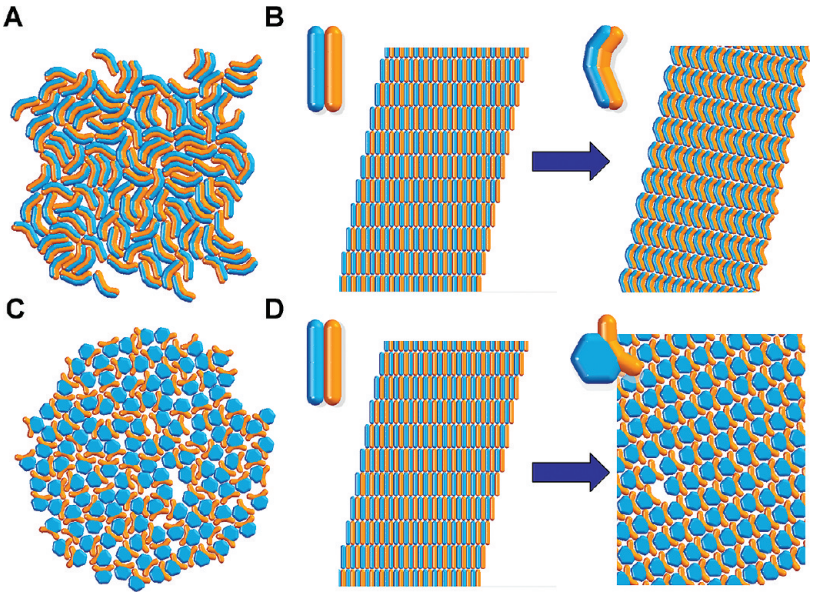

Figure 5. Simulations with biphasic bows and "bull-head" shapes, inspired by ref 12: (A and C) self-assembled structures at $T^* = 0.2$; (B and D) reconfigured structures from a smectic structure of rods at $T^* = 0.2$.

developed an efficient hierarchical method, bottom-up building block assembly (BUBBA), to predict both energy-minimizing[26] and free-energy minimizing[27] structures resulting from the self-assembly of a given set of building blocks. Our self-assembly simulations show that at nonzero temperature, nonconvex shape particles such as L-shaped L4 and L5, hockey sticks, zigzags, T-shaped, cross-shaped, and Y-shaped particles nucleate into precursors of several energy minimum structures as predicted by BUBBA (Figure 6), yet the overall systems are disordered and kinetically trapped. We then attempt to obtain the BUBBA-predicted motifs by transforming preassembled spheres and rods into the target shapes. In most cases, the BUBBA-predicted motifs form with a much longer correlation length as compared to those obtained by self-assembly (Figure 6). For instance, the zigzags Z4 and Z5 pack into the BUBBA-predicted energy-minimizing structure when transformed from rods (Figure 6A,B). For hockey sticks H4 (Figure 6C), BUBBA predicts that the energy minimizing structure contains a mixture of mirror-image motifs, which are energetically identical, suggesting that the assembled structure is likely to be a racemic, kinetically trapped mixture of the two-types of domains. By shifting preassembled rods to hockey sticks, the reconfigured structure attains a uniform handedness. Figure 6D shows that the target structure for Y-shaped particles can be achieved from transforming either preassembled spheres or preassembled rods. We observe certain exceptions: the L-shaped particles obtained by "bending" the rods form close-packed (Figure 5E) and porous ordered patterns (Figure 6F) depending on the length ratio of the branches, L4 or L5, respectively. Both structures have higher potential energies than their BUBBA-predicted counterparts, indicative of kinetically trapped configurations; however, they are stable and reproducible in our simulations. Similar to hockey sticks, the L-shaped particles exhibit a uniform handedness in the reconfigured structure, which is not observed in the self-assembly simulations. The porosity in the structure formed by L-shaped particles L5 results from the particle roughness, with spherical beads attempting to pack efficiently with their neighbors. We find that by judiciously shifting the building block geometry, it is possible to achieve desired ordered structures that are inaccessible to traditional assembly methods.

To assess the relative thermodynamic stability of crystalline structures obtained through reconfiguration, we compare the free energy difference between energy minimizing structures predicted by BUBBA and the corresponding reconfigured structures for several shapes (see the Methods section). As shown in Figure 6G, the difference in the free energy of the reconfigured structures and that of their energy minimizing counterparts is approximately k_BT as $0.2 < T^* < 0.4$. This suggests that the ordered reconfigured structures are as thermodynamically stable as energy minimizing structures in this temperature range.

For $T^* > 0.4$, the reconfigured structures are remarkably less stable than their energy minimizing counterparts for L4 (Figure 6G, top) and H4 particles (Figure 6G, bottom) because the entropy loss due to the particle ordering in reconfigured structures becomes pronounced at high temperature. In contrast, the difference in the free energy of the reconfigured structure from smectic rods and the energy minimizing structure for L5 particles (Figure 6G, bottom) is within k_BT, indicating that these structures are equally thermodynamically stable (within statistical error). Our calculations

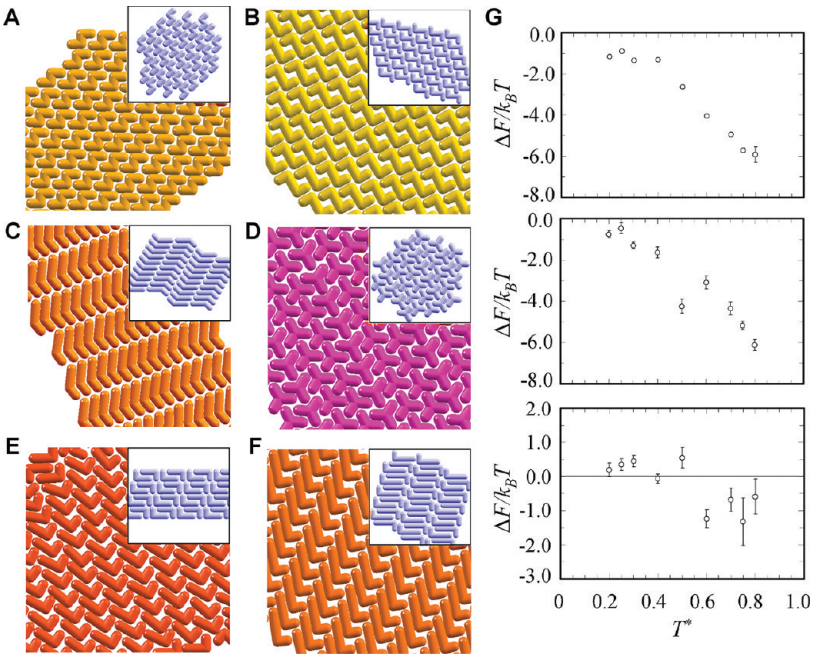

Figure 6. Ordered structures obtained by shape shifting and predicted by BUBBA (inset): (A) zigzags Z4; (B) zigzags Z5; (C) hockey sticks H4; (D) Y-shaped particles Y4; (E) L-shaped particles L4; and (F) L-shaped particles L5. Particles are drawn as smooth for visual clarity. (G) Free energy difference between energy minimizing structures predicted by BUBBA and corresponding reconfigured structures in (C) top; (E) middle; and (F) bottom. Error bars are obtained from five independent samples. In each sample, the free energy difference is averaged over 20 uncorrelated snapshots.

for these particular case studies imply that it is possible to achieve thermodynamically stable structures *via* shape shifting, especially in the low temperature regime, or equivalently, when the attraction strength between the particles is sufficiently strong.

Reconfigurability between Ordered Structures. When the particles in Figure 1 are transformed into spheres the triangular lattice is always recovered regardless of the transformation pathway. We find that direct reconfiguration between ordered structures is reversible when the particle shape is shifted between convex particles such as squares, rhombuses, and pentagons. For backward transformation to rods from rodlike particles such as hockey sticks, L-shaped, and zigzags, the particles should be aligned such that their major axis is kept consistent with the layer direction (Figure 7A); otherwise, the resulting rods, though aligning with their nearest neighbors, do not exhibit any long-range ordering (Figure 7B). Reversible reconfigurations are also found for shape shifting between convex and nonconvex shapes, *e.g.*, between square and Y-shapes, between hockey sticks and zigzags, and between pentagons and crosses. The reconfigurability between ordered structures thus enables us to perform multistep shape shifting based upon current experimental capabilities. For example, if rods cannot be transformed into zigzags directly, we can first transform the rods into hockey sticks, resulting in a biaxial smectic structure as shown in Figure 7C (middle). Subsequently, the hockey sticks may be bent at the longer end, turning into zigzags, which now form the ordered structure as expected (Figure 7C (right)).

Shape shifting can either alter the close-packed packing pattern or toggle between a close-packed and a porous configuration, which might yield bulk materials with interesting optical and mechanical properties. For example, as preassembled spheres grow into squares and crosses, the initial triangular lattice is switched to rhombic lattices (Figures 3A and 3D). The P_2 symmetry packing is also replaced by a rhombic packing when rods are transformed to hockey sticks and L-shaped particles; and the patterns simultaneously turn from uniaxial to biaxial smectic with an additional ordering caused by the nested particles. As another example, Figure 7D shows the pattern reconfiguration occurring in an example of shape shifting in series: preassembled rods → squares → Y-shaped particles Y4 → spheres.

The reconfiguration from a close-packed to a porous morphology can be induced by adjusting the particle aspect ratio. For example, consider the structures formed by Y-shaped particles with different branch lengths (Figure 7E): as the branches are shortened or lengthened, the resulting structures become close-packed or porous, respectively, reminiscent of the opening and closing of a membrane. Unlike the porosity observed with L-shaped particles L5 (Figure 7F), which is caused by the particle bumpiness, the pore size here is twice as large as a subunit bead comprising the particle.

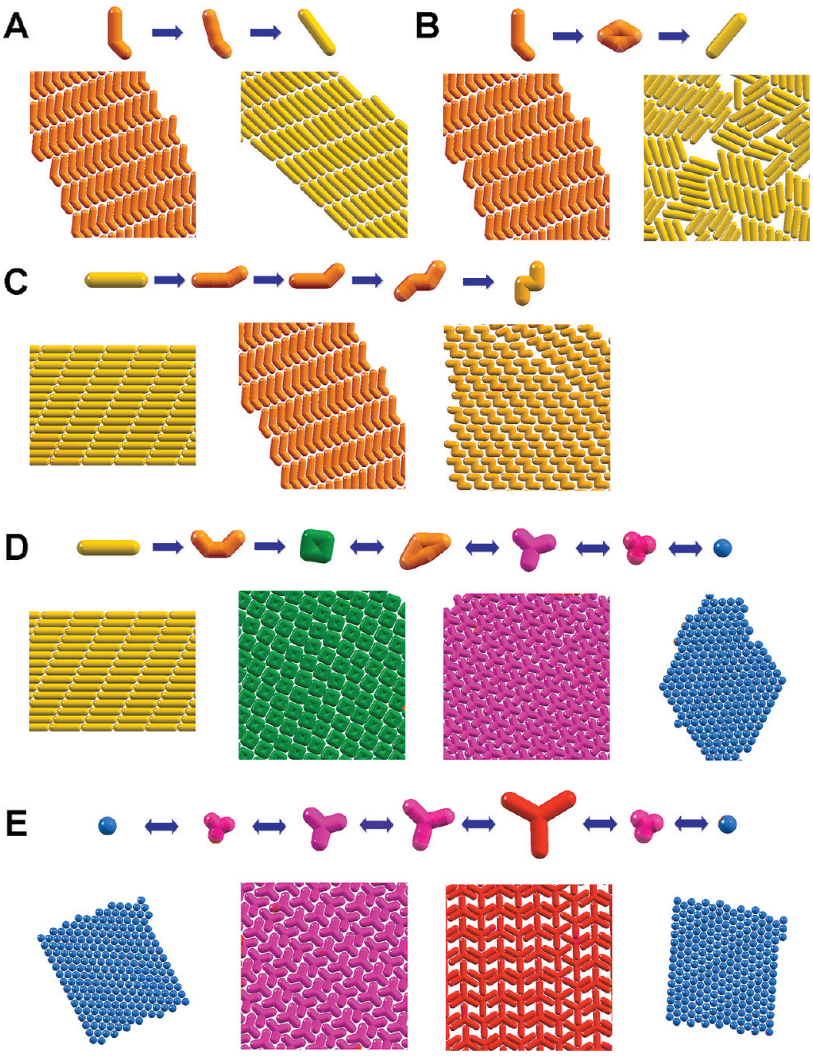

Figure 7. Reconfigurability between ordered structures in sequence: (A) ordered structure obtained when zigzags Z4 are straightened into rods; (B) disordered structure obtained when zigzags Z4 morph into rods through a convex shape; (C) a multistep shape-changing transformation from rod-hockey-zigzag Z4; (D) switching between packing patterns in the sequence of rod → square → Y-shaped Y4 → sphere transformations; and (E) reversible structural morphology change as an opening-closing effect between sphere → Y-shaped Y7 particle with different branch lengths. The shape-shifting pathways are illustrated by snapshots of intermediate shapes from left to right. The arrows indicate shape-shifting directions.

Of significant practical importance, we find that the time required for these structures to reconfigure in response to particle shape change is very short compared to the time required to assemble either structure from isotropic states. Our simulations show that after the shape shifting completes, the order−order reconfiguration completes within 10^6 time steps, considerably faster than the relaxation time required for self-assembly from disordered states, which is on the order of *ca.* 10^7−10^8 time steps. In our simulations, a time step corresponds to approximately 0.001 ns (see the Methods section), meaning that the time scale of the reconfiguration process is in the order of milliseconds. Analogous phenomena could account for the short time scales of some biological assemblies, in which proteins adopt different conformations depending on their local environment. More complicated pathways can be further envisioned by shifting into shapes that easily form ordered structures, for example, spheres and Y-shaped particles, connecting several ordered structures. In parallel with this work, we have proposed a novel methodology to design assembly pathways to increase the self-assembly propensity of strongly interacting building blocks.[27] This methodology can serve to guide to the multistep, shape-changing induced reconfigurations en route to engineering pathways for functional nanostructures.

Shape-Shifting Induced Reconfiguration: A Kinetics-Dependent Process. It is important to address the role of three crucial factors that help determine the formation of target structures in most of the cases studied here: the initial ordered structures, the pathway toward a target shape, and the transformation rate. The initial ordered structures, such as a triangular lattice of spheres or a smectic structure of rods, play an important role in the ordering of the final structures. Unlike self-assembly

from isotropic states, the evolution of the system is biased toward the target structures by the initial configurations of the original building blocks, and purposely so. The natural crystalline ordering of spheres and rods at high densities, which includes the lattice spacing and, in the case of rods, directionality, helps guide the packing of shape-shifted particles. For example, the smectic layers of rods allow the transformed hockey sticks and L-shaped particles to easily pack with adjacent neighbors, leading to biaxial smectic phases (Figure 3E,F); meanwhile, those grown from spheres do not exhibit any long-range ordering. When Y-shaped particles are grown from spheres in a triangular lattice, their three branches are favored to nest with those coming from their six nearest neighbors to form the target configuration (Figure 3D). Since spheres and rods on a flat surface always tend to self-assemble into a triangular lattice and, at sufficiently high densities, a smectic-like structure, respectively, these two ordered structures seem to be reasonable starting points for shape-shifting processes.

The second factor comes from the pathway to transform a particle into a nonconvex target shape. Although, in principle, one can envision various ways to transform a particle shape into one another; our results indicate that the pathway can be strategically selected to optimize long-range ordering in the target structure. As a general heuristic, particle orientation relative to neighboring particles should be consistent with the local packing of the target structure during transformation. We observe that pathways that do not satisfy this condition often give rise to disordered structures (Figure 4), or structures with a shorter range ordering (Figure 7B), both of which are kinetically trapped. For example, to form the ordered structure with zigzags (Figure 6A,B) the rods should be simultaneously bent at two ends in opposite directions to maintain layering. If it is impossible to induce such a direct transformation between two shapes, a pathway can be constructed by carrying out multistep shape transformations as mentioned earlier (*cf.* Figure 7C). Nonetheless, we should emphasize that in this study we have not taken into account any change in the energy scale along the shape-shifting pathway, which likely determines whether the ordering of intermediate states could be sustained.

The third important factor is the transformation rate of the particle shape change, which can affect the long-range ordering, especially of nonconvex target particles. If the particle transformation time is comparable to the system's relaxation time, the influence of the initial ordered structures is significantly reduced. The system evolves in the same manner as the self-assembly of target particles. If the transformation rate is too fast, the target particles form locally ordered clusters with their neighbors, but the system remains disordered on larger length scales because the energy required to rearrange and register the clusters into a crystal is much greater than thermal fluctuations. For example, we observed that a transformation rate of slower than $10^{-4}\sigma$ per time step is required to form the ordered structure of Y-shaped particles from rods. For faster rates, the number of defects in the resulted structures increases and the correlation length decreases substantially.

The significance of these three factors demonstrates that the shape-shifting induced transformation is highly kinetics-dependent, as one might expect. Though the resulting structures may be either free-energy minimizing or kinetically trapped the configurations generated *via* shape shifting are predictable and reproducible provided that the shape transformation pathways are well controlled. For convex target particles such as squares, rhombuses, and pentagons, we find the dependence of the resulting structures on the transformation rates and pathways are less significant. This is because the convex geometry favors the (near) tiling of space, and hence the particles tend toward a close-packed configuration at high densities. In these cases, the quality of the initial ordered structure plays an important role in facilitating reconfiguration to a target crystal structure.

CONCLUSION

Although the shape of particles plays a key role in determining the formation of, and the local packing in, assembled structures, only recently has the possibility arisen to dynamically change the shape of particles on time scales much shorter than required for self-assembly. Because of the large parameter space associated with designing self-assembling systems, especially those with shape-changing particles, computer simulations can provide important insight and design heuristics to guide experiment. We proposed a framework to investigate the effects of particle shape shifting on the self-assembly and reconfigurability of self-assembled structures. The particle model used in this study is a basic model for a large number of shape-changing nanoparticles, colloids, gel-based particles, peptides, and other stimuli-responsive building blocks. By shifting the particle shape dynamically, we showed that one can induce reconfiguration between ordered structures. The resulting structures exhibit longer range ordering, and achieve it on shorter time scales, compared to those attained through traditional self-assembly of the target shape particle. In the examples studied here, we showed that the initial preassembled configuration of rods and spheres, the transformation pathway, and shape-change rate are shown to be crucial factors to the order−order transition in most studied cases. We further showed that, in principle, a pathway to a desired ordered structure, given an initial ordered structure, can be constructed by performing a series of shape changing steps; such methods can be

used to engineer pathways to previously inaccessible regions of phase space. The reconfigurability of assembled structures in our model, mimicking that of biological systems, serves to inspire novel approaches to the fabrication of next-generation functional nanomaterials.

The models and shape-shifting considerations explored here may also prove useful in understanding self-assembly in systems of soft particles where shape fluctuations, rather than on-cue shape changes, occur naturally. In such systems, shape fluctuations may affect the assembly kinetics in ways that could be explored in analogy with the studies we have presented. Despite the simplistic shape shifting considered here, the simulation model and methodology are applicable to more interesting shape changes in 3D, which is the focus of future work.

METHODS

Model. We use a generic phenomenological model interacting with empirical pairwise interactions, similar to those commonly used to model systems of molecules, nanoparticles, and colloids.[28] Each model particle is composed of N_B coarse-grained spherical beads, frozen into rigid bodies. Here we extend previous studies[16−20] to allow these rigid particles to transform into various shapes (Figure 1) during simulations by gradually translating the constituent beads of a particle in the body-fixed coordinates toward target geometries while keeping them rigidly connected. The particles are transformed at the same rate along the same path with respect to the particle body-fixed coordinates. Our model crudely mimics how actual building blocks might react to environment changes such as pH, ionic strength, or directional external field. In this minimal model, we focus mainly on changes in the building block geometry, assuming that material is conserved, and that input energy required for the shape-shifting process does not melt the crystalline structures. Nonconservation of material and local energy changes upon transformation can be included through extensions of our simulation framework for future investigation.

Figure 2 shows the initial two-dimensional ordered structures assembled by spheres (Figure 2A) and rods (Figure 2B) studied in this work. We choose these structures as initial states since they are ubiquitously observed in experimental assemblies of spherical and rodlike particles on a flat interface. For spherical particles, constituent beads (N_B = 4, 5, and 7) are initially placed on top of each other; meanwhile, for rodlike particles (N_B = 4), the center−center distance between adjacent beads is equal to the bead diameter, σ. The target shapes shown in Figure 1 can be divided into two categories: convex (squares, rhombuses, pentagons) and nonconvex shapes, which include rodlike (L-shaped, hockey sticks, zigzags, bows) and branched (cross-shaped, T-shaped, Y-shaped) particles.

In nanoparticle and colloid systems, the effective attraction between the building blocks may have energetic origins such as van der Waals interaction, dipole−dipole interactions, and hydrogen bonding; or entropic origins such as like-charged attraction, hydrophobic interactions, and depletion forces depending on solvent and temperature. In our generic model, the interaction between constituent beads from different particles is modeled by a site−site 12−6 Lennard-Jones potential, truncated and shifted to zero at the distance of 2.5σ. As such, the Lennard-Jones well depth ε characterizes the attraction strength between the constituent beads. The anisotropic nature of the interaction between particles is thus inherently incorporated into the particle geometry without any explicit modification in the force field. The interaction strength (ε) between beads is fixed during the shape-shifting process. Since we seek to understand the role of particle shapes in determining resulted structures, a sufficiently large value of ε that prevents the structures from melting is adequate. Here $\varepsilon > 1.2k_BT$ is shown to be sufficient to induce the aggregation of particles. The representative data shown in the Results and Discussion section are obtained for $\varepsilon = 4.0k_BT$, and a transformation rate of $10^{-5}\sigma$ every 10 time steps is used unless stated otherwise. Examples of shape-shifting processes are given in the Supporting Information.

We employ the general shape-matching algorithm developed by Keys *et al.*[25] to compare the resulted structures from shape transformation and those from self-assembly with corresponding target shapes. The energy minimizing structure in each case is chosen as the reference structure for shape matching comparison. Note that the shape descriptor used for calculating the shape-matching order parameter is determined based on the characteristic length scale of specific structures. For example, for smectic structures formed by hockey sticks H4, the characteristic length is approximately the distance between two adjacent layers. The shape-matching order parameter S varies in [0.0; 1.0] where S = 1.0 indicates a perfect match. The time evolutions of S for several shape-shifting processes are given in the Supporting Information.

Simulation Method. We use Brownian Dynamics, a stochastic molecular dynamics method to simulate the evolution of an isothermal system of particles on a two-dimensional surface with periodic boundary conditions. The implicit solvent molecules serve as a heat bath for the system by exerting random forces and drag forces on each spherical bead comprising the particles. More details on the BD simulation method may be found in ref 29.

At each time step, the beads in each particle are moved together as a rigid object. We vary the transformation rate, or equivalently, the number of time steps to complete the shape transformation, and perform multiple independent runs to verify the robustness of our results. After the particles adopt their target shapes, the simulations run until the structure reaches an apparently stable state. The system sizes are small enough to achieve equilibration in a reasonable amount of time and large enough to avoid finite size effects in the local structures. A typical simulation consists of N_P = 225 particles, each containing N_B = 4, 5, or 7 beads. Since we do not consider the system at high pressure, this system size is sufficient to observe regular packing patterns and to avoid finite size effects.

We perform simulations of particles in their target shapes from disordered states at instantaneous temperature to compare the resulting structures and those obtained from shape shifting. In these simulations, we attempt to overcome kinetic traps by frequently annealing the system. Our simulations are conducted using HOOMD-blue,[30] our group's open source molecular dynamics code optimized for graphics processing units, and LAMMPS,[31] an open source molecular dynamics code using a LAMMPS extension we developed for this work that allows three-dimensional rigid bodies to change their geometry during simulations.

Free-Energy Calculations. To investigate the relative thermodynamic stability of the ordered structures resulting from shape shifting as compared to those predicted by BUBBA for the target shapes at a given temperature, we use the lattice-coupling-expansion method[32,33] to calculate the excess free energy of the structures under consideration with respect to their reference Einstein crystals. We note that relevant free-energy calculation methods are also mentioned elsewhere.[34,35] The potential energy used for thermodynamic integration in the coupling stage is[33]

$$\tilde{U}(\mathbf{r}^{N_P}, \mathbf{Q}^{N_P}, \lambda) = U(\mathbf{r}^{N_P}, \mathbf{Q}^{N_P}) + \lambda \sum_{i=1}^{N_P} (k_t(\mathbf{r}_i - \mathbf{r}_{i0})^2 + k_r \sin^2 \theta_i)$$

where N_P is the number of particles, and k_t and k_r are the translational and rotational spring constants, respectively. The external potential is composed of translational and rotational terms. The translational term couples the particle center of mass with a lattice site. The rotational term biases the particle orientation toward a preferential direction in the crystal. During the coupling stage, λ is varied from 0 to 1 to transform from the original structure to a structure in which the particles are "tethered" to the lattice sites and their orientation is constrained to the preferred orientation. θ_i is the angle of the orientation of the particle i from its preferred orientation, extracted from the change in the quaternion from the original orientation: $\Delta\mathbf{Q} = \mathbf{Q}^{-1}\mathbf{Q}_0$ where $\mathbf{Q}_0$ and $\mathbf{Q}$ are the original and instantaneous quaternions, respectively. The free-energy change in the coupling stage is given by[33]

$$\Delta F_1 = \int_0^1 \left\langle \frac{\partial \tilde{U}}{\partial \lambda} \right\rangle_\lambda \mathrm{d}\lambda = \int_0^1 \langle \sum_{i=1}^{N_P} (k_t(\mathbf{r}_i - \mathbf{r}_{i0})^2 + k_r \sin^2 \theta_i) \rangle_\lambda \mathrm{d}\lambda$$

Once the coupling stage is completed, the particles (and their lattice sites) are moved apart by a box size expansion. During the expansion stage, the parameter γ is increased from 1 corresponding to the initial box size until the virial vanishes. The expansion is considered complete when the interaction virial is effectively zero. The free energy change in the expansion stage is given by[29]

$$\Delta F_2 = \int_1^\infty \langle \sum_{i=1}^{N} \sum_{j \neq i}^{N} -\mathbf{f}_{ij} \cdot \mathbf{r}_{ij}^0 \rangle_\gamma \mathrm{d}\gamma$$

where $\mathbf{r}_{ij}^0$ is the initial separation between two particles i and j. The excess free energy difference between the original ordered structure and the Einstein crystal is then determined by the sum of ΔF_1 and ΔF_2: $\Delta F = F - F_{Ein} = -(\Delta F_1 + \Delta F_2)$. During the coupling and expansion stages, the system is equilibrated at constant temperature using the Nose–Hoover thermostat. The ensemble average is performed by averaging over 20 equilibration snapshots within each step of λ and γ. The free energy of molecular Einstein crystals, which can be determined analytically, is identical for different crystals of the same shape.[32,33]

Acknowledgment. The authors thank Carolyn Phillips, Kevin Kohlstedt, Michael Engel, Aaron Keys, Amir Haji-Akbari, Daniel Ortiz and Benjamin Schultz for helpful discussions. The authors acknowledge support from the James S. McDonnell Foundation 21st Century Science Research Award/Studying Complex Systems under Award No. 220020139. This material is also based upon work supported by the Department of Defense, the Office of Director, Defense Research and Engineering (DOD/DDRE) under Award No. N00244-09-1-0062. Any opinions, findings, and conclusions or recommendations expressed in this publication are those of the author(s) and do not necessarily reflect the views of the DOD/DDRE. This material is based upon work supported by, or in part by, the U.S. Army Research Office under Grant Award No. W911NF-10-1-0518. S.C.G. is grateful to the University of Michigan Center for Advanced Computing for cluster support. T.D.N. acknowledges the Vietnam Education Foundation. This research was made possible, in part, by Government support under and awarded by the Department of Defense, Air Force Office of Scientific Research, National Defense Science and Engineering Graduate (NDSEG) Fellowship, 32 CFR 168a (E.J.).

Supporting Information Available: Examples of shape-shifting pathways and time evolution of shape shifting order parameter. This material is available free of charge *via* the Internet at http://pubs.acs.org.

REFERENCES AND NOTES

1. Bishop, J.; Burden, S.; Klavins, E.; Kreisberg, R.; Malone, W.; Napp, N.; Nguyen, T. Programmable Parts: A Demonstration of the Grammatical Approach to Self-Organization. *Int. Conf. Intell. Robots Syst.* **2005**, 3684–3691.
2. Klavins, E. Programmable Self-Assembly. *IEEE Control Syst. Mag.* **2007**, *27*, 43–56.
3. Chang, S.-S.; Shih, C.-W.; Chen, C.-D.; Lai, W.-C.; Wang, C. R. C. The Shape Transition of Gold Nanorods. *Langmuir* **1999**, *15*, 701–709.
4. Link, S.; Burda, C.; Nikoobakht, B.; El-sayed, M. A. Laser-Induced Shape Changes of Colloidal Gold Nanorods Using Femtosecond and Nanosecond Laser Pulses. *J. Phys. Chem. B* **2000**, *104*, 6152–6163.
5. Link, S.; Wang, Z. L.; El-sayed, M. A. How Does a Gold Nanorod Melt? *J. Phys. Chem. B* **2000**, *104*, 7867–7870.
6. Kim, J.-K.; Lee, E.; Lim, Y.-B.; Lee, M. Supramolecular Capsules with Gated Pores from an Amphiphilic Rod Assembly. *Angew. Chem., Int. Ed.* **2008**, *47*, 4662–4666.
7. Lee, E.; Kim, J.-K.; Lee, M. Reversible Scrolling of Two-Dimensional Sheets from the Self-Assembly of Laterally Grafted Amphiphilic Rods. *Angew. Chem., Int. Ed.* **2009**, *48*, 3657–3660.
8. Chockalingam, K.; Blenner, M.; Banta, S. Design and Application of Stimulus-Responsive Peptide Systems. *Protein Eng., Des. Select.* **2007**, *20*, 155–161.
9. Gebhardt, K. E.; Ahn, S.; Venkatachalam, G.; Savin, D. A. Rod-Sphere Transition in Polybutadiene-poly(L-lysine) Block Copolymer Assemblies. *Langmuir* **2007**, *23*, 2851–2856.
10. Gebhardt, K. E.; Ahn, S.; Venkatachalam, G.; Savin, D. A. Role of Secondary Structure Changes on the Morphology of Polypeptide-Based Block Copolymer Vesicles. *J. Colloid Interface Sci.* **2008**, *317*, 70–76.
11. Yoo, J.-W.; Mitragotri, S. Polymer Particles That Switch Shape in Response to a Stimulus. *Proc. Natl. Acad. Sci. U.S.A.* **2010**, *107*, 11205–11210.
12. Lahann, J. Shape-Switching Multi-compartmental Particles. Private communication, August 15, 2011.
13. Glotzer, S. C.; Solomon, M. J. Anisotropy of Building Blocks and Their Assembly into Complex Structures. *Nat. Mater.* **2007**, *6*, 557–562.
14. Yang, Z.; Huck, W. T. S.; Clarke, S. M.; Tajbakhsh, A. R.; Terentjev, E. M. Shape-Memory Nanoparticles from Inherently Non-spherical Polymer Colloids. *Nature* **2005**, *4*, 486–490.
15. Nolte, P.; Stierle, A.; Jin-Phillipp, N. Y.; Schulli, T. U.; Dosch, H. Shape Changes of Supported Rh Nanoparticles During Oxidation and Reduction Cycles. *Science* **2008**, *321*, 1654–1658.
16. Zhang, Z. L.; Glotzer, S. C. Tethered Nano Building Blocks: Toward a Conceptual Framework for Nanoparticle Self-Assembly. *Nano Lett.* **2003**, *3*, 1341–1346.
17. Horsch, M. A.; Zhang, Z. L.; Glotzer, S. C. Simulation Studies of Self-Assembly of End-Tethered Nanorods in Solution and Role of Rod Aspect Ratio and Tether Length. *J. Chem. Phys.* **2006**, *125*, 184903–12.
18. Nguyen, T. D.; Zhang, Z. L.; Glotzer, S. C. Molecular Simulation Study of Self-Assembly of Tethered V-Shaped Nanoparticles. *J. Chem. Phys.* **2008**, *129*, 244903–11.
19. Iacovella, C. R.; Glotzer, S. C. Phase Behavior of Ditethered Nanospheres. *Soft Matter* **2009**, *5*, 4492–4498.
20. Horsch, M. A.; Zhang, Z. L.; Glotzer, S. C. Self-Assembly of End-Tethered Nanorods in a Neat System and Role of Block Fractions and Aspect Ratio. *Soft Matter* **2010**, *6*, 945–954.
21. Batista, V. M. O.; Miller, M. A. Crystallization of Deformable Spherical Colloids. *Phys. Rev. Lett.* **2010**, *105*, 088305–4.
22. Zhang, Y.; Lu, F.; Lelie, D.; Gang, O. Continuous Phase Transformation in Nanocube Assemblies. *Phys. Rev. Lett.* **2011**, *107*, 135701.
23. Nguyen, T. D.; Glotzer, S. C. Reconfigurable Assemblies of Shape-Changing Nanorods. *ACS Nano* **2010**, *4*), 2585–2594.
24. Schilling, T.; Pronk, S.; Mulder, B.; Frenkel, D. Monte Carlo Study of Hard Pentagons. *Phys. Rev. E* **2005**, *71*, 036138–6.
25. Keys, A. S.; Iacovella, C. R.; Glotzer, S. C. Characterizing Structure through Shape Matching and Applications to Self-Assembly. *Annu. Rev. Condens. Matter Phys.* **2011**, *2*, 263–285.

26. Jankowski, E.; Glotzer, S. C. A Comparison of New Methods for Generating Energy-Minimizing Configurations of Patchy Particles. *J. Chem. Phys.* **2009**, *131*, 104104–8.
27. Jankowski, E.; Glotzer, S. C. Assembly Pathway Engineering: Designing Patchy Particles for Self-Assembly Propensity. Unpublished work.
28. Glotzer, S. C.; Solomon, M. J.; Kotov, N. A. Self-Assembly: From Nanoscale to Microscale Colloids. *AIChE J.* **2004**, *50*, 2978–2985.
29. Frenkel, D.; Smit, B., *Understanding Molecular Simulation from Algorithms to Applications*; Academic Press: San Diego, CA, 2002.
30. Anderson, J. A.; Lorenz, C. D.; Travesset, A. General Purpose Molecular Dynamics Simulations Fully Implemented on Graphics Processing Units. *J. Comput. Phys.* **2008**, *227*, 5342–5359.
31. Plimpton, S. J. Fast Parallel Algorithms for Short-Range Molecular Dynamics. *J. Comput. Phys.* **1995**, *117*, 1–19.
32. Vlot, M. J.; Huinink, J.; Eerden, J. P. v. d. Free Energy Calculations on Systems of Rigid Molecules: An Application to the TIP4P Model of H_2O. *J. Chem. Phys.* **1999**, *110*, 55–61.
33. Noya, E. G.; Conde, M. M.; Vega, C. Computing the Free Energy of Molecular Solids by the Einstein Molecule Approach: Ices XIII and XIV, Hard-Dumbbells and a Patchy Model of Proteins. *J. Chem. Phys.* **2008**, *129*, 104704–16.
34. Haji-Akbari, A.; Engel, M.; Glotzer, S. C. Degenerate Quasicrystal of Hard Triangular Bipyramids. **2011**, *arXiv:1106.5561v1 [cond-mat.stat-mech]*. http://arxiv.org/abs/1106.5561.
35. Haji-Akbari, A.; Engel, M.; Glotzer, S. C. Phase Diagram of Hard Tetrahedra. **2011**, *arXiv:1106.4765v2 [cond-mat.soft]*. http://arxiv.org/abs/1106.4765.